

Defect Evolution Mechanism and Quantitative Criteria in Thread Rolling of Ti-6Al-4V Bolts

Xiangwei Zhang¹, Ni Zhen¹, Rui Ye², Liangliang Wei^{2,*}

¹ School of Mechanical Engineering, Tianjin University of Science and Technology, Tianjin, 300222, China

² Key Laboratory of Fastening and Connecting Technology Enterprises of Tianjin, Aerospace Precision Industry Co., Ltd, Tianjin, 300300, China

*Corresponding author

Keywords: Ti-6Al-4V, Thread Rolling, Forming Instability, Burr Defects, Quantification Criteria

Abstract: Thread rolling of titanium alloys is an important process for improving the fatigue resistance of aerospace fasteners. However, under high-speed processing conditions, unstable material flow may lead to severe surface burr defects. This study investigates the influence of rolling speed on thread forming quality and defect evolution in Ti-6Al-4V bolts using DEFORM-3D simulations and experiments. The results show that increasing rolling speed gradually drives the forming process into an unstable state, where burr distribution evolves from localized defects on the thread flank to continuous material overflow at the thread root. To quantitatively characterize this failure process, a multi-dimensional evaluation criterion is proposed based on the speed fluctuation standard deviation (δ_v) and cumulative slip index (D_s). The results indicate that δ_v determines the frequency and intensity of burr formation, whereas D_s governs the physical depth of burr growth. This study provides a quantitative basis for defect prediction and process optimization in titanium alloy thread rolling.

1. Introduction

Titanium alloys (Ti-6Al-4V) are widely used in critical aerospace and high-end fasteners due to their high specific strength, excellent corrosion resistance, and good high-temperature mechanical properties[1-2]. Compared with traditional cutting, thread rolling offers higher production efficiency and better material utilization [3-5]. The process aligns the metal fibers along the thread profile and introduces residual compressive stress in the surface layer[6-9], significantly improving bolt fatigue life and tensile strength[10-12].

However, under high-speed rolling conditions, non-uniform material flow and surface burr defects easily occur, which have attracted considerable research attention. In numerical simulation studies, Chen et al.[13] established a three-dimensional finite element model using DEFORM-3D and simulated nonlinear material flow under friction constraints. Hsia et al.[14] optimized the mesh strategy through convergence analysis and predicted the stress-strain distribution during thread

forming. Zhang et al. [15] developed a 3D finite element model for round-die thread cold rolling, revealing metal flow trajectories and radial load evolution, and showed that plastic deformation is mainly concentrated in the surface layer near the thread profile. In terms of process parameter effects and forming quality prediction, Domblesky and Feng [16] systematically analyzed the key influences of billet diameter, friction conditions, and die geometry on forming quality[16]. Giorleo et al. [17] focused on the impact of flat die geometry parameters on workpiece accuracy, providing theoretical support for process design. Regarding the formation mechanism of defects, Nitu et al. [18] analyzed the material damage laws in unsteady plastic deformation; Volz et al. [19] pointed out that stroke rate and lubrication system are critical factors inducing interface slip; Groche and Kramer [20-21] further elucidated the influence of driving parameters on forming stability, laying the foundation for understanding the process limits in complex plastic flow.

Despite these studies, quantitative evaluation of kinematic instability in high-speed rolling of strain-rate-sensitive titanium alloys remains limited. In particular, the relationship between billet motion instability, interfacial slip, and burr defect evolution has not been clearly quantified. This study establishes a quantitative kinematic instability criterion for thread rolling based on measurable velocity fluctuations and cumulative slip behavior. Two indicators, namely the speed fluctuation standard deviation (δ_v) and the cumulative slip index (D_s), are proposed to characterize instantaneous motion instability and cumulative interfacial sliding during the forming process. This approach provides a quantitative framework for linking kinematic instability with burr defect evolution and offers theoretical guidance for optimizing high-speed thread rolling of titanium alloy fasteners.

2. Numerical and experimental setup

This section describes the numerical and experimental methods used in this study. It covers the establishment of the rolling finite element model, the selection of key parameters, and the corresponding experimental verification process.

2.1 Numerical model

The MJ5×0.8 bolt, widely utilized as a fastener in mechanical equipment, was selected as the rolling workpiece. The material is Ti-6Al-4V, and its specific parameters are detailed in Table 1.

Table 1: Material property parameters

Material	Modulus of elasticity (GPa)	Tensile strength (MPa)	Yield strength (MPa)	Poisson's ratio
Ti-6Al-4V	113	895	855	0.3

The finite element model consists of a cylindrical billet and two parallel thread-forming dies, as shown in Figure 1. The dies were modeled as rigid bodies to enhance computational efficiency. The key geometric dimensions of the model are as follows in Table 2.

The numerical simulation was performed using DEFORM-3D software for three-dimensional rigid-plastic finite element analysis. The billet was meshed using tetrahedral elements. Considering that thread forming mainly occurs at the surface of the billet and defects frequently appear on the surface, the mesh density in the surface region of the billet was refined (Figure 1b). In the contact region, the minimum mesh size was set to 0.05 mm to more accurately capture the details of material flow.

Table 2: Geometric dimensions of the model

Parameter	Setting
Static die length	158mm
Moving die length	177mm
In-press angle/Out-press angle α_0	1.5 °
Thread profile angle α	60 °
Thread height H	0.425mm
Pitch P	0.8mm
Billet diameter	4.43mm
Billet length	6mm

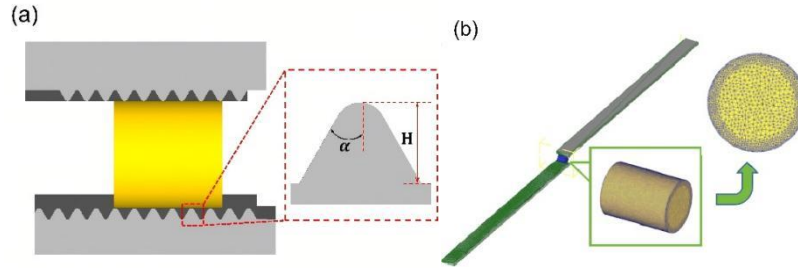


Figure 1: (a) 3D finite element model (b) Mesh generation of the billet surface layer

Since the rolling contact time is extremely short and the speed is high, in this study, frictional heat generation and thermo-mechanical coupling are neglected, and uses a shear friction model (Eq. 1) to characterize the high-speed nonlinear interface contact characteristics.

According to the shear factor model, frictional stresses can be expressed as shown in Eq. 1:

$$\tau = m k \quad (1)$$

In the formula, k is the shear flow stress of the workpiece, and m is the dimensionless constant friction coefficient.

Friction boundary conditions have a significant impact on the accuracy of numerical simulations in cold forming. Zhang et al. [22] evaluated the effectiveness of different characterization schemes by comparing four types of cold extrusion friction tests, while Müller [23] explored the improvement mechanisms of interface friction with a single-layer lubrication system. However, existing studies mostly focus on stable forming processes and are not directly applicable to high-speed rolling conditions. Therefore, this study calibrates the friction parameters by inversely determining the friction parameters through the geometric profile of the thread cross-section.

Table 3 shows additional information regarding the configuration of the numerical model.

Table 3: Simulation parameters of thread rolling process

Parameter	Setting
Friction condition	$m=0.30, 0.50$
Forming temperature	Room temperature
Infeeding speed of moving die	550~650mm/s
Radial travel	340mm
Number of elements in the billet	390000

2.2 Experimental setup

Thread rolling experiments were conducted on a CPR-6S flat-die thread rolling machine, using billets consistent with the simulation model. The static die was fixed to the machine base, while the moving die translated tangentially along the X-direction (Figure 2a). The static die consisted of the inlet zone (IZ), calibration zone (CZ), and discharge zone (DZ).

At the initial stage, the moving die contacted the billet and gradually indented it. The forming load was applied by reducing the die gap, driving billet rotation and axial feeding. The thread was then finished in the calibration zone to ensure dimensional accuracy. Finally, the workpiece exited through the outlet zone and detached from the dies, completing the rolling process.

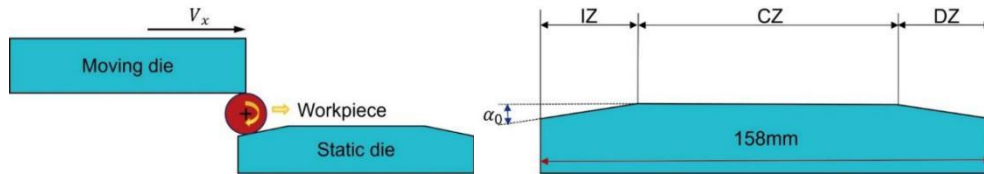


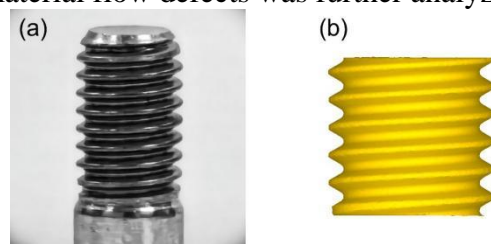
Figure 2: (a) Schematic of the thread rolling process; (b) Schematic diagram of a cross-section of a static die

To investigate the effect of moving-die rolling speed on metal flow defects and to validate the simulation results, thread rolling experiments were conducted at speeds of 50–56 r/min. Each condition was repeated at least five times to ensure reliability.

Thread surface morphology was scanned along the crest axis using a KC-X1000 laser confocal microscope. The maximum burr height and burr area ratio were extracted to quantitatively evaluate rolling defects.

3. Friction calibration

The friction model parameters were validated by comparing the thread geometry from simulations and experiments. The experimental result (Figure 3a) shows good agreement with the simulated geometry (Figure 3b). Based on this validation, the effect of moving-die rolling speed on the formation and evolution of material flow defects was further analyzed.



(a) Experimental result (b) FEM results

Figure 3: Comparison of rolled shape of thread (MJ5 × 0.8)

Unlike conventional cold forging processes, thread rolling simulations typically employ higher friction coefficients to ensure the stable rotation of the workpiece. By comparing the simulation results with the experimental profile cross-section under different friction coefficients ($m=0.3$ and $m=0.5$), it was found that the profiles from both methods exhibit good consistency (Figure 4).

Table 4 compares the simulated profiles with experimental profiles under different friction coefficients ($m=0.3$ and $m=0.5$), focusing on evaluating the pitch (P), thickness (T), and height (H) of a single thread segment. The analysis shows that the predicted P and H from both models match

well with the experimental results. However, for T prediction, Model 1 ($m=0.3$) exhibits a significant deviation from the experimental values, which is attributed to the idealized die angle in the simulation, differing from the actual geometry affected by manufacturing tolerances. In contrast, Model 2 ($m=0.5$) shows errors of less than 3% across all dimensional indicators (Table 4), validating the accuracy of the high-friction model in the numerical simulation of thread rolling.

Table 4: Forming profile error analysis under different friction coefficients

Dataset	Pitch (P , μm)	Thickness (T , μm)	Height (H , μm)	Diff P (%)	Diff T (%)	Diff H (%)
Model 1($m=0.3$)	808	366	447	+1	-10	+6
Model 2($m=0.5$)	803	395	429	+1	-3	+2
Experimental	798	406	420			

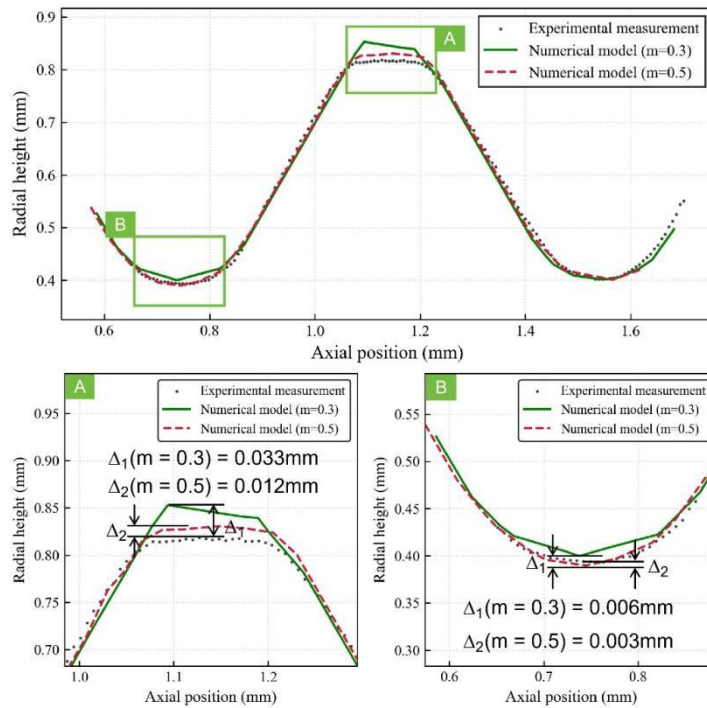


Figure 4: Comparison of experimentally measured and numerically calculated workpiece geometry

In the root area, the simulation results of both models ($m=0.3$ and $m=0.5$) are in high agreement with the experimental profiles, with the maximum deviation ranging from 0.003 to 0.006 mm, indicating that root forming is mainly governed by die geometry constraints. However, in the crest area, the effect of the friction coefficient on metal flow behavior is significant: the low-friction model ($m=0.3$) exhibits noticeable overfilling, with a height deviation of up to 0.033 mm, while the high-friction model ($m=0.5$) shows a deviation of only 0.012 mm, and its predicted crest morphology is much closer to the experimental results. This further confirms the superiority of the high-friction model in accurately reflecting the actual metal flow behavior, particularly in controlling the H and crest shape.

4. Analysis of Kinematic instability and defect evolution

4.1 Velocity evolution of billet during rolling

The ideal state of the flat die thread rolling process follows a pure rolling mechanism (Figure 5),

where the billet undergoes uniform plastic deformation driven by the static frictional force between the static and moving dies. The linear speed of the moving die is set to V_{die} , and according to the principle of the instantaneous center of rotation, the translational speed $V_{workpiece}$ at the center of the billet should theoretically be exactly half of the moving die speed (Eq. 2)

$$V_{workpiece} = \frac{V_{die}}{2} \quad (2)$$

In this state, the die profile symmetrically presses into the surface layer of the billet, and the material subjected to radial extrusion flows radially toward the thread crest, thereby filling the die cavity.

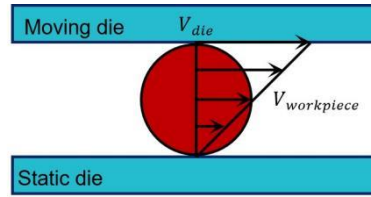


Figure 5: Schematic of ideal pure rolling mechanism in flat-die thread rolling

In the actual forming process, it is extremely difficult to maintain pure rolling balance. Due to the high yield strength and significant work hardening characteristics of Ti-6Al-4V, the tangential resistance at the die and workpiece contact interface often deviates from the theoretical driving force provided by the frictional force. This dynamic imbalance leads to a deviation between the actual translational speed and the theoretical speed, resulting in a slip phenomenon. The instantaneous velocity mismatch $\Delta_V(t)$ is defined as:

$$\Delta_V(t) = V_{workpiece} - \frac{V_{die}}{2} \quad (3)$$

When the tangential resistance is too large, the actual speed will be significantly lower than the theoretical value; conversely, during certain stages of motion, the actual speed may exceed the theoretical speed. This velocity mismatch disrupts the symmetrical pressing state of the thread profile, which is the core cause of material asymmetrical flow and the subsequent formation of burr defects.

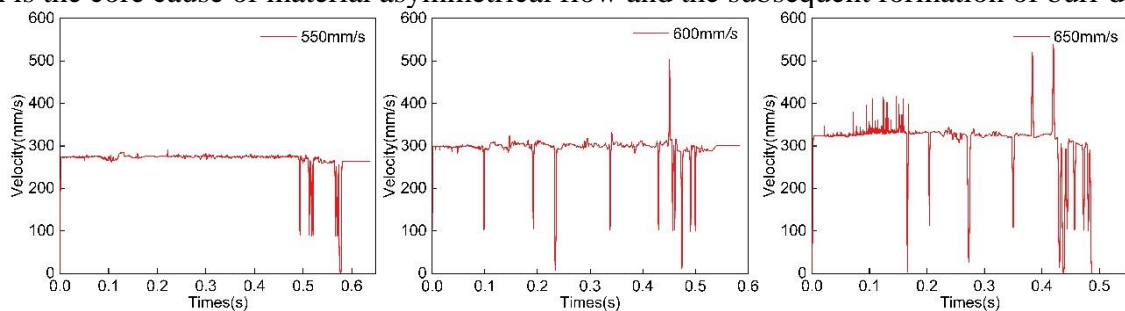


Figure 6: Evolution of billet center velocity at different rolling speeds

Further analysis of the kinematic response of the billet center at different moving die speeds is shown in Figure 6. As the speed increases from 550 mm/s to 650 mm/s, the stability of the billet center velocity significantly deteriorates. At 550 mm/s, the velocity curve remains smooth and closely follows the theoretical value, indicating stable pure rolling. Only in the discharge zone (DZ) does the velocity fluctuate due to the billet gradually disengaging from the die, with limited impact on forming quality.

However, at higher speeds, the velocity curve shows high-frequency, large-amplitude fluctuations, indicating that extreme instantaneous slip between interfaces increases, causing frequent deviations

from the ideal motion trajectory.

4.2 Experimental results

This study used a profilometer to capture the morphology of threads at different speeds (Figure 7) and analyzed the frequency of various burr morphologies at different speeds (Figure 8). Based on experimental observations and statistical analysis, the thread forming quality was divided into three typical process intervals according to the processing speed:

4.2.1 Stable forming interval (50 r/min)

At this speed, the threads exhibit excellent surface integrity. 3D morphology confirms complete metal filling with no significant overflow. Statistical data (Figure 8) shows that Burr-free samples have an 80% frequency, with only minor defects near the thread crest. According to Groche et al., geometric deviations near the crest are generally considered secondary defects with limited impact on fatigue life. However, defects in the stress-concentrated root area can easily evolve into crack sources, significantly reducing load-bearing capacity²⁰.

4.2.2 Medium-speed transition interval (51 – 53 r/min)

As speed increases, burrs begin to form on the flank and migrate toward the root, often appearing as intermittent local protrusions. The proportion of Burr-free samples decreases, while the frequency of flank burrs rises. The physical cause is microscopic slip at the contact interface: strong shear forces cause the surface metal to be dragged upward along the die surface. Material flow remains in a quasi-steady state.

4.2.3 High-speed instability interval (54–56 r/min)

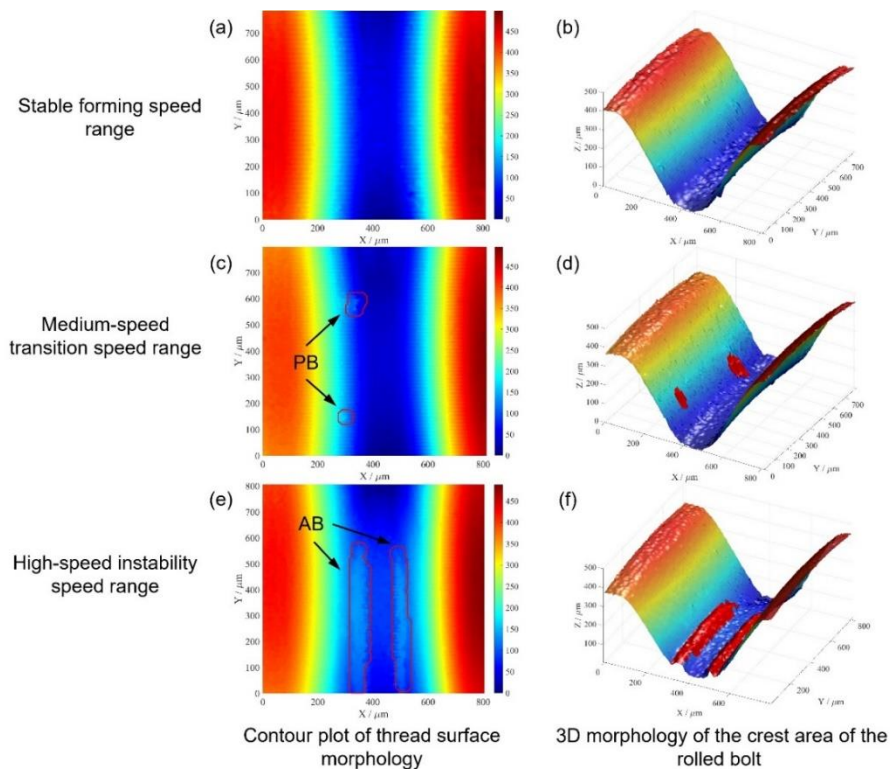


Figure 7: Profilometric analysis of thread topography; PB: Point-like burr; AB: Area-like burr

In this range, the processing system enters a significant unstable state, and burr growth points undergo a dramatic change. Local burrs on the flank quickly decrease, replaced by explosive surface overflow in the root area. Statistical results show that Burr-free samples disappear completely, indicating a loss of control over the material flow path.

From the morphological evolution trajectory (Figure 7), the defects transition from localized point-like to continuous surface-like forms. This abrupt morphological change reflects a significant increase in instantaneous slip intensity. Interface friction instability under high-speed rolling induces severe instantaneous slip, causing the die to deviate from the intended rolling path and subjecting the formed flank to a cutting-type extrusion. This disrupts thread forming regularity, leading to disordered migration of the metal away from the preset filling path.

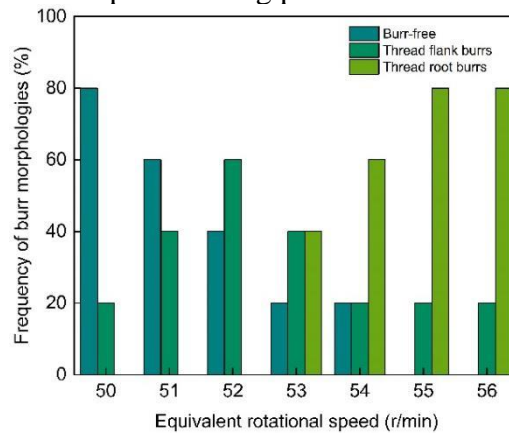


Figure 8: Thread defect distribution vs. rolling speed

4.3 Displacement evolution and slip-induced defect formation

The previous section revealed the macroscopic evolution of defects from the perspective of process parameters. This section focuses on the time history of a single forming process, analyzing the initiation and propagation mechanisms of slip defects during the pressing and finishing stages from the perspective of motion stability.

To further reveal the billet slippage and material flow patterns during the rolling process, tracking points were set in the characteristic regions of the thread tooth segment (Figure 9), and the displacement evolution process of the material from the initial stage to the end of forming was analyzed under the condition of a moving die speed of 600 mm/s.

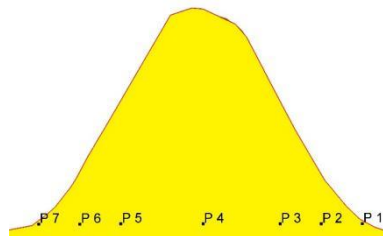


Figure 9: Tracking point schematic

4.3.1 Forming stage division and displacement evolution

Analysis of Figure 10a and the triaxial displacement evolution curves (Figures 10b, c, and d) shows that the billet underwent approximately 11 cycles of extrusion forming during the flatbed rolling process (Figures 10b and 10d). The axial (Y-direction) displacement of the material exhibits significant staged evolution characteristics (Figure 10c).

(1) Pressing Stage($t < t1$):

The billet passes through the die inlet zone (IZ), and the die teeth gradually cut into the billet surface. By time $t1$, the billet has completed rolling in the inlet zone and enters the calibration zone.

(2) Finishing Stage($t1 \leq t < t2$):

Initially, the die gap remains constant in the calibration zone (CZ). The billet undergoes approximately 1~2 rotation cycles to finish the geometric defects formed in the pressing stage, and the system is in a quasi-steady-state operating range.

(3) Steady-State Operating Stage($t \geq t2$):

Theoretically, this stage should tend towards a pure rolling state, but due to interface slip, each tracking point still exhibits axial displacement (Figures 10a and 10c). Observations show that slip causes continuous axial slippage at each point; especially at time $t3$, extreme instantaneous slippage occurs, causing drastic changes in axial displacement and completely disrupting the stability of material flow.

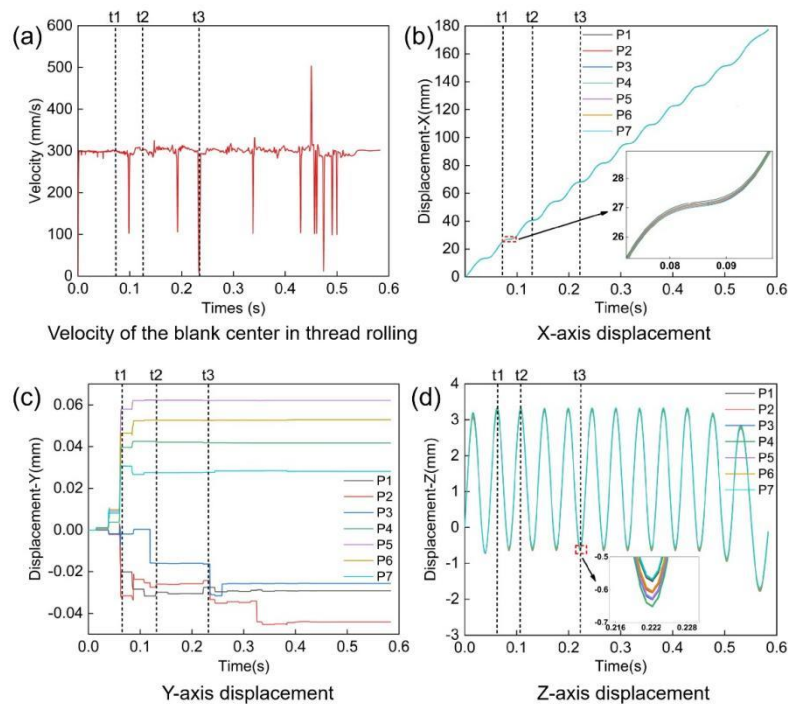


Figure 10: Displacement evolution of tracking points during thread rolling

4.3.2 Slip defect formation mechanism

This section, combining the fluctuation of the billet center velocity with the displacement law of the thread tooth cross-section tracking point, quantitatively reveals the formation mechanism of the tooth root surface material overflow caused by tooth flank cutting extrusion due to extreme instantaneous slippage, and clarifies why it is difficult to correct in subsequent rolling processes.

The billet center velocity is not constant at 300 mm/s, but fluctuates frequently within the range of 296~302 mm/s (Figure 10a). The material rheological inconsistencies caused by this slippage can be corrected by subsequent die pressure. However, there is a significant moment of dynamic instability during the rolling process ($t=t3$), when the billet center velocity drops sharply, causing violent relative sliding between the die and the workpiece. The tooth flank material migrates along the Y-axis and accumulates at the inlet and outlet of the contact area. When there is excessive accumulation at the outlet, the material is subjected to strong extrusion after entering the stationary die, and excess metal overflows at the tooth root corner, ultimately forming defects such as burrs or cracks.

The motion trajectory of the subsurface tracer point $P2$ verifies this mechanism: during the finishing stage ($t2 \sim t3$), its axial displacement is only a slight change of 0.0031 mm; however, when the velocity drops sharply at time $t3$, the axial displacement of point $P2$ increases sharply by 0.0108 mm in a very short time, an increase of approximately 3.5 times that of the finishing stage.

Since this phenomenon occurs in the later stage of forming, when the material's plasticity has significantly decreased, the resulting defects cannot be eliminated by subsequent rolling, becoming the core issue in the forming quality of titanium alloy bolts.

5. Quantitative criteria for instability evaluation

5.1 Definition of instability indicators

To accurately quantify the degree of slippage during thread rolling and reveal its impact on forming quality, this section defines the following two types of core indicators based on the principle of kinematic stability to evaluate the cumulative effect and instantaneous fluctuation characteristics of slippage:

(1) Cumulative slip index (D_S)

Since defect formation is influenced by both instantaneous damage and the degree of turbulence throughout the forming path, this study introduces the D_S to describe the cumulative effect within the rolling cycle. This index is defined as the integral of the absolute value of the instantaneous speed mismatch over the rolling time T :

$$D_S = \int_0^T |\Delta_V(t)| dt \quad (4)$$

This indicator represents the total relative sliding displacement between the die teeth and the workpiece surface, reflecting the repeated shearing action on the material surface. A higher value means that the blank has undergone more frequent sliding within the die cavity, usually indicating a greater risk of surface tearing.

(2) Speed fluctuation standard deviation (δ_V)

δ_V is a core quantitative indicator characterizing the stability of billet movement. It is used to evaluate the degree of dispersion of the actual speed from the theoretical speed. The calculation formula is:

$$\delta_V = \sqrt{\frac{1}{N-1} \sum_{i=1}^N (V_i - \frac{V_{de}}{2})^2} \quad (5)$$

In the formula, N represents the number of velocity sampling points, and V_i represents the actual velocity of the billet center at the i -th sampling moment. A larger δ_V indicates stronger kinematic instability, more severe velocity fluctuations, and a greater likelihood of material flow turbulence.

5.2 Evolution of instability indicators

To verify the applicability of the proposed criteria under different conditions, this section compares and analyzes the slip characteristics from numerical simulations with the burr evolution observed experimentally. As shown in Figure 11a, within the simulation speed range of 550 to 650 mm/s, both D_S and δ_V exhibit significant positive monotonic growth, indicating that an increase in rolling speed intensifies the instantaneous slip behavior between the die and the billet. The experimental results (Figure 11b) highly match the simulation trend: when the speed increases from 50 r/min to 56 r/min (566.7 ~ 634.7 mm/s), the burr averages (height (h), area ($S\%$)) increase non-linearly with speed.

Comparing Figures 11a and 11b, the evolution trends of the numerical simulation indicators (D_s, δ_v) and the experimental defect characteristics ($h, S\%$) are highly synchronized. Notably, after the 54 r/min (600 mm/s) threshold, both show a significant change in growth slope. This strong agreement effectively confirms the feasibility of using interface kinematic indicators to predict titanium alloy thread forming defects.

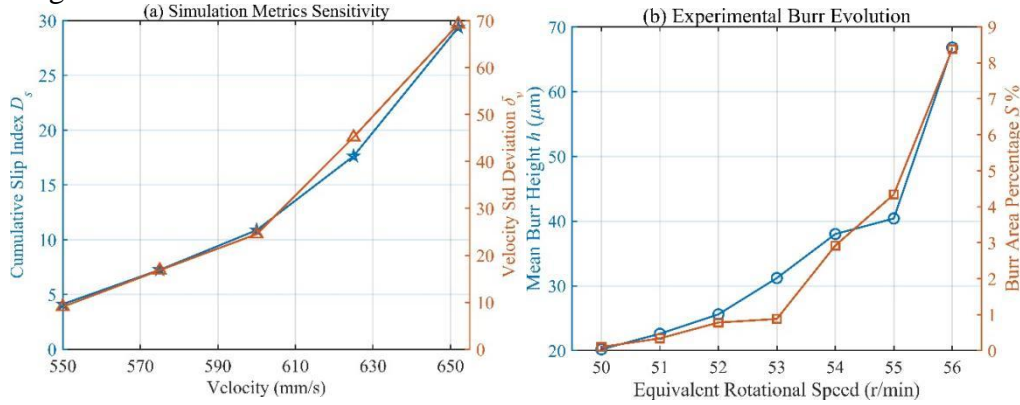


Figure 11: (a) Evolution of simulation metrics (b) Experimental burr evolution

5.3 Correlation with burr defects

To further quantify and validate the predictive effect of physical indicators on burr defects, this study analyzes the consistency between simulation indicators and experimental data using 50 r/min (566.7 mm/s) as the baseline condition. Figure 12 shows that the goodness of fit (R^2) for all indicator combinations is above 0.91, indicating a strong linear correlation between simulation indicators and actual forming quality.

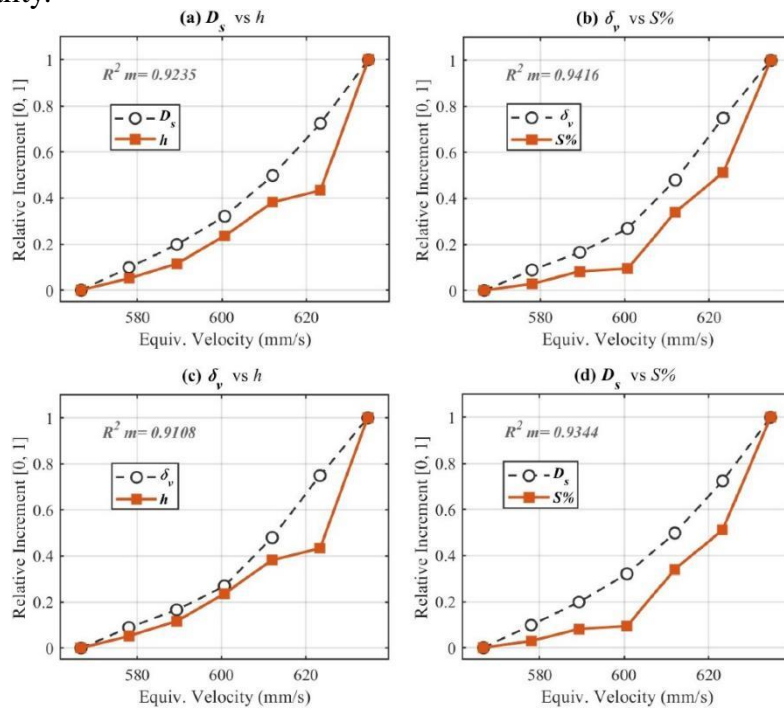


Figure 12: Correlation analysis

Among all evaluation combinations, δ_v showed the most significant correlation with $S\%$ ($R^2=0.9235$). This indicator determines the frequency and severity of extreme instability phenomena.

Since the cutting extrusion induced by sudden velocity changes is instantaneous, its impact on material flow expands to the surrounding area as dynamic instability intensifies, thus determining the distribution area of burrs. Therefore, δ_V can serve as a key indicator for predicting the generation of planar burrs.

D_S shows a strong correlation with burr height h ($R^2=0.9235$), indicating that it is the core factor driving burr longitudinal growth. The mechanism is as follows: D_S reflects the cumulative effect of frictional shear force on the continuous pulling of surface metal. The larger the slip, the more metal deviates from the preset filling path. Due to the rigid space constraints of the thread profile, excess metal cannot be effectively contained and is extruded outward along the die gap, thus dominating the longitudinal growth depth of the burr.

The fitting accuracy of each index combination remains high, indicating that this multidimensional criterion system can robustly describe complex plastic flow defects. The high correlation among the main criterion combinations reveals the different roles played by each criterion in physical characterization. δ_V defines the frequency and extent of burr formation, while D_S controls the physical depth of burr growth. Together, they provide a complete quantitative description of the forming quality of titanium alloy threads from the perspectives of instantaneous strength and cumulative effect.

6. Conclusions

This study investigated the instability behavior and burr defect evolution during flat-die thread rolling of Ti-6Al-4V bolts through numerical simulation and experimental observations.

The results reveal a clear evolution pattern of burr defects associated with billet motion instability. At relatively stable rolling conditions, burrs first appear as localized point-like protrusions along the thread flank. As the rolling speed increases and the instability becomes more pronounced, slip between the dies and the billet intensifies, leading to excessive material accumulation in the thread root. Consequently, the burr morphology gradually transforms from discrete flank-side points into continuous surface overflow along the thread root. This transition indicates that burr formation is governed by the progressive accumulation of slip-induced material flow.

To quantitatively characterize this behavior, two instability indicators were introduced: the velocity fluctuation standard deviation (δ_V) and the cumulative slip index (D_S). The results show that δ_V is strongly correlated with the burr area, reflecting the frequency and spatial extent of burr initiation caused by instantaneous motion instability. In contrast, D_S shows a strong correlation with burr height, indicating the cumulative material extrusion that controls the growth depth of burr defects.

Compared with previous studies that mainly focused on stress distribution, forming load, or geometric accuracy of the thread profile, the present work provides a new perspective by linking burr morphology evolution to kinematic instability and interfacial slip behavior.

From an engineering perspective, controlling velocity fluctuation and cumulative slip is essential for reducing burr defects. The proposed indicators provide a practical method for evaluating process stability and optimizing high-speed thread rolling of titanium alloy fasteners.

References

- [1] Mei, M., Zhao, Y. and Chen, C., *Extrusion internal thread of titanium alloy plate: Multi-objective optimization of material flow-induced defects. Proceedings of the Institution of Mechanical Engineers, Part E: Journal of Process Mechanical Engineering*, 2025, 09544089251343974.
- [2] Maciel, D. T., Filho, S. L. M. R., Lauro, C. H. and Brandão, L. C., *Characteristics of machined and formed external threads in titanium alloy. The International Journal of Advanced Manufacturing Technology*, 2015, 79, 779–792.
- [3] Tschaetsch, H., *Metal forming practise: processes—machines—tools. Springer*, 2006.
- [4] Song, J., Liu, Z. and Li, Y., *Cold rolling precision forming of shaft parts. Springer*, 2017.

- [5] Zhou, Q., & Zhang, J. (2024). Numerical simulation study on the cold thread rolling forming of Ti-6Al-4V alloy fasteners with external threads and their defects. In *Journal of Physics: Conference Series* (Vol. 2815, No. 1, p. 012028). IOP Publishing.
- [6] Furukawa, A., & Hagiwara, M. (2015). Estimation of the residual stress on the thread root generated by thread rolling process. *Mechanical Engineering Journal*, 2(4), 14-00293.
- [7] Martin, J. A. (1998). *Fundamental finite element evaluation of a three dimensional rolled thread form: Modelling and experimental results* (No. KAPL-P--000058; K--98003; CONF-980708--). Knolls Atomic Power Lab., Schenectady, NY (United States).
- [8] Du Maire, P., Hoffmeister, J., Johlitz, M. and Öchsner, A., Influence of the manufacturing process on the fatigue strength of threads. *Materialwissenschaft und Werkstofftechnik*, 2025, 56, 638–645.
- [9] Maurya, A., Hwang, J.-W., Yeom, J.-T., Kim, J. H., Yang, J., Kim, J. H., Lim, J., Lee, S. W., Park, C. H. and Hong, J. K., Optimized Process Design for Uniform Microstructure and High-Strength Ti-6Al-4 V Alloy Fasteners in Aerospace Applications. *Metals and Materials International*, 2025, 1–13.
- [10] Oberg, E., Jones, F. D., Horton, H. L., Ryffel, H. H. and McCauley, C. J., *Machinery's handbook*. Industrial press New York, 2004.
- [11] Kim, W., Kawai, K., Koyama, H. and Miyazaki, D., Fatigue strength and residual stress of groove-rolled products. *Journal of Materials Processing Technology*, 2007, 194, 46–51.
- [12] Zhang, D.-W., Zhao, S.-D. and Ou, H., Analysis of motion between rolling die and workpiece in thread rolling process with round dies. *Mechanism and Machine Theory*, 2016, 105, 471–494.
- [13] Chen, C. H., Wang, S. T. and Lee, R. S., 3-D finite element simulation for flat-die thread rolling of stainless steel. *Journal of the Chinese Society of Mechanical Engineers, Transactions of the Chinese Institute of Engineers, Series C/Chung-Kuo Chi Hsueh Kung Ch'eng Hsuebo Pao*, 2005, 26, 617–622.
- [14] Hsia, S. Y., Pan, S. K., & Chou, Y. T. (2015). Computer simulation for flat-die thread rolling of screw. In *International Conference on Innovation, Communication and Engineering*.
- [15] Zhang, D.-W., Zhang, C., Tian, C. and Zhao, S.-D., Forming characteristic of thread cold rolling process with round dies. *The International Journal of Advanced Manufacturing Technology*, 2022, 120, 2503–2515.
- [16] Domblesky, J. P. and Feng, F., A parametric study of process parameters in external thread rolling. *Journal of Materials Processing Technology*, 2002, 121, 341–349.
- [17] Giorleo, L. and Cartapani, M., Influence of die threading and finishing length in the thread-rolling process using flat dies: a numerical analysis. *Journal of The Institution of Engineers (India): Series C*, 2022, 103, 403–411.
- [18] Nitu, E., Tabacu, S., Iordache, M. and Iacomi, D., Finite element analysis and experimental validation of the wedge rolling process. *Proceedings of the Institution of Mechanical Engineers, Part B: Journal of Engineering Manufacture*, 2013, 227, 1325–1339.
- [19] Volz, S. and Groche, P., Experimental investigation on slip conditions during thread rolling with flat dies. *Friction*, 2024, 12, 136–143.
- [20] Groche, P. and Kramer, P., Numerical investigation of the influence of frictional conditions in thread rolling operations with flat dies. *International Journal of Material Forming*, 2018, 11, 687–703.
- [21] Kramer, P. and Groche, P., Defect detection in thread rolling processes—experimental study and numerical investigation of driving parameters. *International Journal of Machine Tools and Manufacture*, 2018, 129, 27–36.
- [22] Zhang, Q., Arentoft, M., Bruschi, S., Dubar, L. and Felder, E., Measurement of friction in a cold extrusion operation: Study by numerical simulation of four friction tests. *International Journal of Material Forming*, 2008, 1, 1267–1270.
- [23] Müller, C., *Schmierung von Werkzeugen der Kaltmassivumformung mit Einschichtschmierstoffsystemen*. Shaker, 2015.